Unimolecular Decomposition of Chemically Activated Pentatetraene ($H_2CCCCCH_2$) Intermediates: A Crossed Beams Study of Dicarbon Molecule Reactions with Allene

Ying Guo,[†] Xibin Gu,[†] Fangtong Zhang,[†] Alexander M. Mebel,[‡] and Ralf I. Kaiser*[,†]

Department of Chemistry, University of Hawai'i at Manoa, Honolulu, Hawaii 96822, and Department of Chemistry and Biochemistry, Florida International University, Miami, Florida 33199

Received: April 20, 2006; In Final Form: July 6, 2006

The reactions dynamics of the dicarbon molecule C_2 in the $^1\Sigma_g^+$ singlet ground state and $^3\Pi_u$ first excited triplet state with allene, $H_2CCCH_2(X^1A_1)$, was investigated under single collision conditions using the crossed molecular beam approach at four collision energies between 13.6 and 49.4 kJ mol^{-1}. The experiments were combined with ab initio electronic structure calculations of the relevant stationary points on the singlet and triplet potential energy surfaces. Our investigations imply that the reactions are barrier-less and indirect on both the singlet and the triplet surfaces and proceed through bound C_5H_4 intermediates via addition of the dicarbon molecule to the carbon−carbon double bond (singlet surface) and to the terminal as well as central carbon atoms of the allene molecule (triplet surface). The initial collision complexes isomerize to form triplet and singlet pentatetraene intermediates ($H_2CCCCCH_2$) that decompose via atomic hydrogen loss to yield the 2,4-pentadiynyl-1 radical, $HCCCCCH_2(X^2B_1)$. These channels result in symmetric center-of-mass angular distributions. On the triplet surface, a second channel involves the existence of a nonsymmetric reaction intermediate ($HCCCH_2CCH$) that fragments through atomic hydrogen emission to the 1,4-pentadiynyl-3 radical [$C_5H_3(X^2B_1)HCCCHCCH$]; this pathway was found to account for the backward scattered center-of-mass angular distributions at higher collision energies. The identification of two resonance-stabilized free C_5H_3 radicals (i.e., 2,4-pentadiynyl-1 and 1,4-pentadiynyl-3) suggests that these molecules can be important transient species in combustion flames and in the chemical evolution of the interstellar medium.

Introduction

Cumulenes ($H_2C_nH_2$; $n > 2$) and the corresponding cumulene carbenes (C_nH_2; $n > 2$) present important reaction intermediates in combustion flames,[1] chemical vapor deposition,[2] and in interstellar environments (cold molecular clouds such as TMC-1, circumstellar envelopes of IRC + 10216, and planetary nebulae such as CRL 618).[3] Whereas all cumulene carbenes hold a C_{2v} symmetry and depict $^1A_1$ electronic ground states, the situation for the cumulenes is more complex.[4] Here, molecules having an even number of carbon atoms belong to the D_{2h} point group, whereas an odd number of carbon atoms dictate an inherent D_{2d} symmetry. This correlates with the ^1A_g and $^1A_1$ electronic ground states of the even- and odd-numbered cumulenes, respectively.[5,6] The structures of the cumulenes also correlates with recent studies of ^{13}C nuclear magnetic resonance (NMR) paramagnetic shielding constants.[7] Because of their unique electronic structure, cumulenes also hold important technical potential as elements for molecular machines;[8] the cationic forms serve as models for molecular wires.[9]

Despite the importance of cumulenes in the chemical evolution of extreme environments (combustion flames, CVD, interstellar medium) and promising technological applications, surprisingly little is known about the unimolecular decomposition and hence stability of chemically activated cumulenes. The breakdown of chemically activated singlet and triplet allene (H_2CCCH_2) complexes has been studied previously in crossed beams experiments of electronically excited ($C(^1D)$)[10] and ground state ($C(^3P)$)[11] carbon atoms with ethylene (C_2H_4; X^1A_g); likewise, butatriene intermediates (H_2CCCCH_2) in their singlet ground and electronically excited states were prepared under single collision conditions via the reactions of dicarbon, $C_2(X^1\Sigma_g^+/a^3\Pi_u)$, with ethylene. In all cases, the dynamics of the allene and butatriene decomposition were dominated by atomic hydrogen loss pathways, forming the propargyl (C_3H_3-(X^2B_2)) and the 1-butene-3-yne-2-yl radical (i-$C_4H_3(X^2A')$), respectively. In this paper, we expand these studies and investigate the unimolecular decomposition of chemically activated pentatetraene molecules ($H_2CCCCCH_2$) as synthesized under single collision conditions in crossed beam experiments of dicarbon, $C_2(X^1\Sigma_g^+/a^3\Pi_u)$, with allene ($H_2CCCH_2$; X^1A_1). These studies are pooled together with electronic structure calculations to provide a comprehensive picture of the chemical reaction dynamics and underlying stability of singlet and triplet pentatetraene.

Experimental Setup and Data Analysis

The scattering experiments were conducted under single collision conditions in a crossed molecular beams machine at The University of Hawai'i.[12] Pulsed dicarbon beams were produced in the primary source by laser ablation of graphite at 266 nm[13] (30 Hz). The ablated species were seeded in neat carrier gas (neon and helium; 99.9999%; 4 atm) released by a Proch-Trickl pulsed valve. After passing a skimmer, a four-slot chopper wheel selected a part out of the dicarbon beam at

* Corresponding author. Tel.: (808) 956-5731; fax: (808) 956-5908; e-mail: kaiser@gold.chem.hawaii.edu.
[†] University of Hawai'i at Manoa.
[‡] Florida International University.

10.1021/jp062447l CCC: $33.50
Published on Web 08/24/2006

TABLE 1: Peak Velocities (v_p), Speed Ratios (S), and Center-of-Mass Angles (Θ_{CM}), Together with Nominal Collision Energies of Dicarbon and Allene Reactants (E_c)

beam	v_p (ms^{-1})	S	E_c (kJ mol^{-1})	Θ_{CM}
$H_2CCCH_2(X^1A_1)$	840 ± 3	11.4 ± 0.2		
$C_2(X^1\Sigma_g^+/a^3\Pi_u)$/Ne	1050 ± 6	5.7 ± 0.2	13.6 ± 0.1	53.1 ± 0.2
$C_2(X^1\Sigma_g^+/a^3\Pi_u)$/Ne	1682 ± 22	3.2 ± 0.1	26.5 ± 0.6	39.8 ± 0.4
$C_2(X^1\Sigma_g^+/a^3\Pi_u)$/He	2090 ± 38	4.3 ± 0.3	38.1 ± 1.2	33.8 ± 0.5
$C_2(X^1\Sigma_g^+/a^3\Pi_u)$/He	2426 ± 40	3.9 ± 0.2	49.4 ± 1.5	30.0 ± 0.4

a peak velocities v_p between 1050 ± 6 and 2426 ± 40 ms^{-1}; speed ratios from 3.2 ± 0.1 to 5.7 ± 0.2 were obtained (Table 1). Note that at these velocities, the beam contains dicarbon in its $X^1\Sigma_g^+$ electronic ground and in its first excited $a^3\Pi_u$ state;[13] the energy separation between both states is only 8.6 kJ mol^{-1}. Note that the dicarbon beam has not been characterized via laser induced fluorescence; therefore, the relative contribution of dicarbon in its electronic ground state versus its first electronically excited state is unknown. The segments of the dicarbon beam crossed a pulsed allene beam (H_2CCCH_2; 99.6%; 520 Torr; $v_p = 840 \pm 3$ ms^{-1}; $S = 11.4 \pm 0.2$) released by a second pulsed valve perpendicularly under well-defined collision energies between 13.6 ± 0.1 and 49.4 ± 1.5 kJ mol^{-1} in the interaction region. The ablation beam also contains carbon atoms and tricarbon molecules. However, the latter do not interfere with the scattering signal of the dicarbon−allene reaction at mass-to-charge ratios (m/z) of 63 ($C_5H_3^+$) to 60 (C_5^+). Tricarbon was found to react with allene only at collision energies larger than 63 ± 3 kJ mol^{-1}.[14] A signal from the reaction of atomic carbon with allene shows up at m/z values of 51 ($C_4H_3^+$) and lower.[15] The reactively scattered species are monitored using a quadrupole mass spectrometric detector in the time-of-flight (TOF) mode after electron-impact ionization of the molecules. This detector can be rotated within the plane defined by the primary and secondary reactant beams to take angular resolved TOF spectra. By integrating the TOF spectra at distinct laboratory angles, we obtain the laboratory angular distribution (i.e., the integrated signal intensity of an ion of distinct m/z versus the laboratory angle). Information on the chemical dynamics was extracted by fitting these TOF spectra and the angular distribution in the laboratory frame (LAB) using a forward-convolution routine.[16] This approach initially assumes an angular distribution $T(\theta)$ and a translational energy distribution $P(E_T)$ in the center-of-mass reference frame (CM). TOF spectra and the laboratory angular distribution were then calculated from these center-of-mass functions. The final outcome is the generation of a product flux contour map, which reports the differential cross section, $I(\theta,u)$, of the product of the intensity as a function of angle θ and product center-of-mass velocity u. This map contains all the details of the scattering process.

Theoretical Procedures

The reactants, products, various intermediates, and transition states on the potential energy surfaces for the $C_2(X^1\Sigma_g^+)$/$C_2(a^3\Pi_u)$ plus allene reactions have been optimized using the hybrid density functional B3LYP method with the 6-311G(d,p) basis set.[17,18] Vibrational frequencies also have been calculated at the B3LYP/6-311G(d,p) level for the characterization of stationary points (number of imaginary frequencies NIMAG = 0 and 1 for local minima and transition states, respectively) and to obtain zero point energy (ZPE) corrections. The energies were then refined by single point calculations using the G2M-(CC,MP2) method,[19] which approximates the coupled cluster[20] CCSD(T)/6-311+G(3df,2p) energy. All calculations were carried out using the GAUSSIAN 98[21] and MOLPRO 2000[22] programs. In this paper, we only focus on the computational results to supplement the experimental data. The complete triplet and singlet C_5H_4 surfaces will be released in a forthcoming publication.

Results

Reactive Scattering Signal and TOF Spectra. The reactive scattering signal was detected at mass-to-charge ratios m/z = 63 ($C_5H_3^+$), 62 ($C_5H_2^+$), 61 (C_5H^+), and 60 (C_5^+). Time-of-flight spectra (TOF) for various scattering angles at the most intense mass-to-charge value (i.e., $m/z = 62$ ($C_5H_2^+$)) are shown in Figure 1 for all four collision energies. We would like to emphasize that at each collision energy investigated, the TOF spectra recorded at mass-to-charge ratios between 63 and 60 are superimposable. This indicates that $m/z = 63$ fragments in the electron impact ionizer also give signals at $m/z = 62-60$. Here, a signal at $m/z = 62$ ($C_5H_2^+$) is more intense by a factor of 1.3 as compared to $m/z = 63$. These identical patterns of the lower mass-to-charge ratios further imply that—at least within this mass range—solely the dicarbon versus hydrogen replacement channel can take place. This pathway leads to the synthesis of C_5H_3 isomer(s) ($m/z = 63$) plus atomic hydrogen; the formation of any C_5H_2 isomer(s) ($m/z = 62$) together with the molecular hydrogen counter fragment can be ruled out. Accounting for the signal-to-noise level, upper limits of the molecular hydrogen elimination channel of 1−2% were derived. A signal at a mass-to-charge ratio of $m/z = 52$ ($C_4H_4^+$) is absent, implying that the pathway to form C_4H_4 plus atomic carbon from a potential C_5H_4 is not present. Time-of-flight spectra recorded from $m/z = 51$ ($C_4H_3^+$) to 48 (C_4^+) did not overlap with those at $m/z = 63-60$. Here, TOF spectra in the range of $m/z = 51-48$ had to be fit with two channels: one contribution from the reaction of dicarbon with allene (dissociative ionization of C_5H_3 in the electron impact ionizer) and a second channel from the reaction of atomic carbon with allene forming atomic hydrogen and the 1-buten-3-yn-2-yl radical (i-$C_4H_3(X^2A')$); the latter is also responsible for a signal at $m/z = 51$ (the $C_4H_3^+$ parent) and the fragments at $m/z = 50$ ($C_4H_2^+$), 49 (C_4H^+), and 48 (C_4^+). Summarized, the interpretation of the TOF data verifies the presence of a dicarbon versus atomic hydrogen replacement channel leading to C_5H_3 isomer(s) under single collision conditions at each collision energy.

Laboratory Angular Distributions (LAB). Figure 2 depicts the most probable Newton diagrams of the reactions of dicarbon $C_2(X^1\Sigma_g^+/a^3\Pi_u)$ with allene at all four collision energies together with the laboratory angular distributions (LAB) of the heavy C_5H_3 product recorded at the most intense mass-to-charge ratio of $m/z = 62$ ($C_5H_2^+$). These LAB distributions are spread over 40−50° in the scattering plane defined by both reactant beams. The rather small angular spreads propose that only a comparatively small fraction of the total available energy is channeled into the translational degrees of freedom of the C_5H_3 + H reaction products. This correlates also with the relatively narrow TOF spectra showing a signal only between 300 and 500 μs. Note that the overall shape of the LAB distribution changes with rising collision energy. Although all distributions peak close to the center-of-mass angles of the reactions (Table 1), only the LAB distribution at the lowest collision energy of 13.6 kJ mol^{-1} depicts almost a forward−backward symmetric shape. As the collision energy increases, the distributions become more backward scattered with respect to the dicarbon beam.

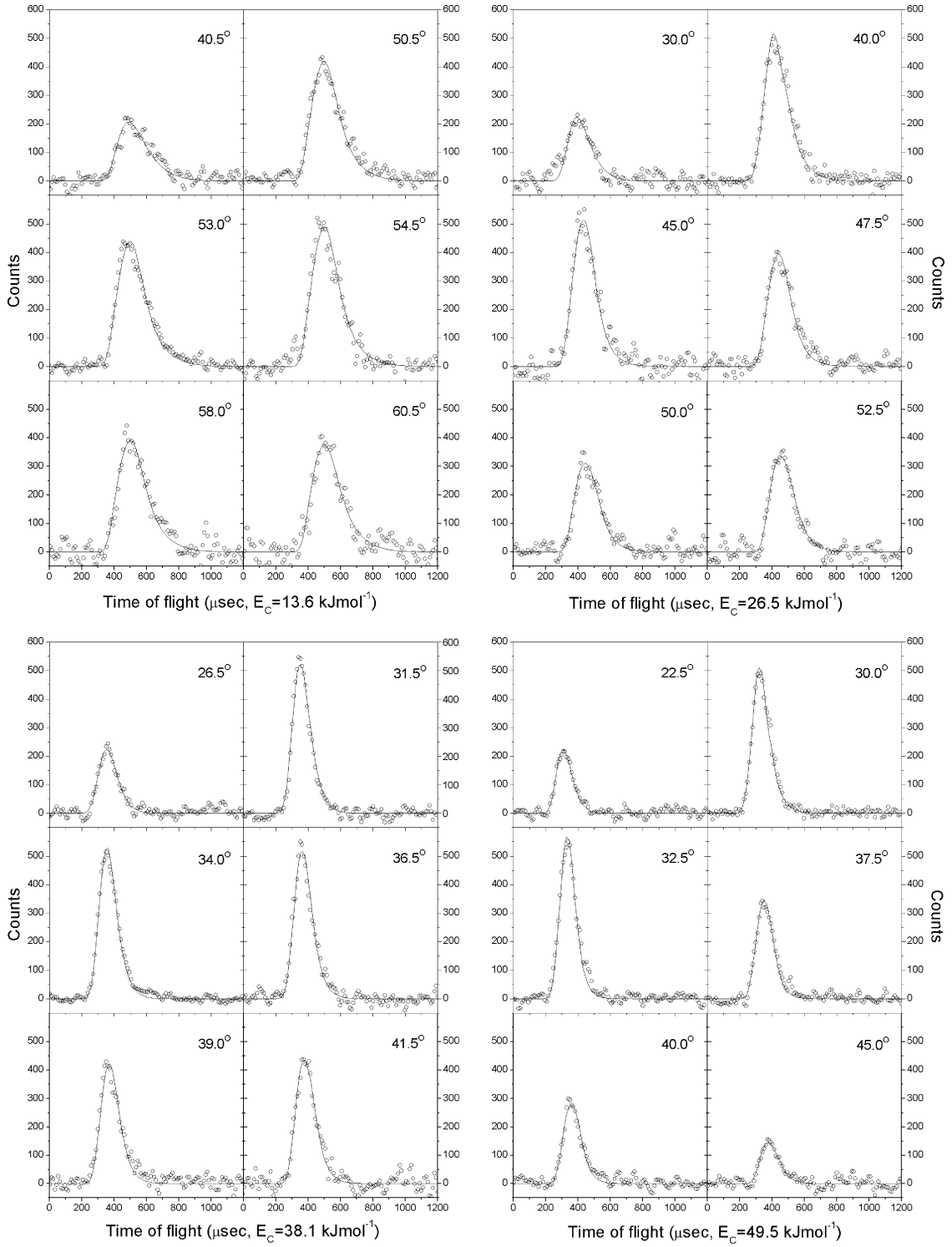

Figure 1. Selected time-of-flight data for $m/z = 62$ ($C_5H_2^+$) recorded at four collision energies at various laboratory angles. The circles indicate the experimental data and the solid lines the calculated fit.

Center-of-Mass Translational Energy Distributions, $P(E_T)$s. The translational energy distributions in the center-of-mass frame, $P(E_T)$, are shown in Figure 3. Here, best fits of the LAB distributions and of the TOF spectra were obtained with only one $P(E_T)$ at each collision energy extending to a maximum translational energy, E_{max}, of 205 kJ mol^{-1} ($E_c = 13.6$ kJ mol^{-1}), 210 kJ mol^{-1} ($E_c = 26.5$ kJ mol^{-1}), 220 kJ mol^{-1} ($E_c = 38.1$ kJ mol^{-1}), and 225 kJ mol^{-1} ($E_c = 49.4$ kJ mol^{-1}). It should be emphasized that because of the emission of a light hydrogen atom, the derived fits are relatively insensitive to the high-energy cutoff. Here, extending or cutting the tail by ±15 kJ mol^{-1} did not influence the quality of the fit as evident from the almost invariant χ^2 parameter. For those molecules without internal excitation, the maximum translational energy portrays the collision energy plus the reaction energy. Therefore, E_{max} aids in calculating the reaction exoergicity. Averaging over all four collision energies, we find that the formation of the C_5H_3 radical(s) and atomic hydrogen is exoergic by 183 ± 15 kJ mol^{-1}. In the most favorable case, the most probable translational energy presents an order-of-magnitude of the barrier height in the exit channel. In the present distributions, all $P(E_T)$s show a plateau between 3 and 40 kJ mol^{-1}. These data suggest

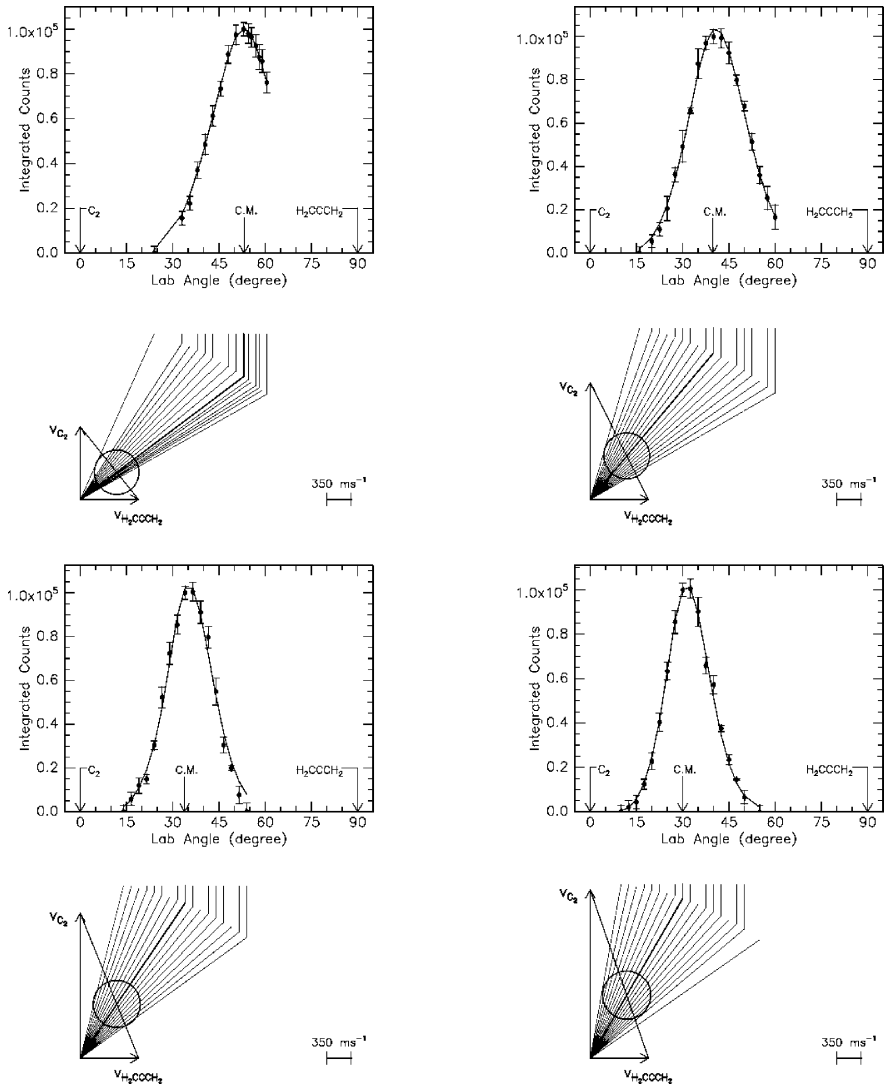

Figure 2. Newton diagrams for the reaction of dicarbon molecules with allene at four collision energies of 13.6 (top left), 26.5 (top right), 38.1 (bottom left), and 49.4 kJ mol^{-1} (bottom right) together with the corresponding laboratory angular distribution of the C_5H_3 radical(s) recorded at $m/z = 62$. Circles and error bars indicate experimental data, and the solid line indicates the calculated distribution with the best-fit center-of-mass functions.

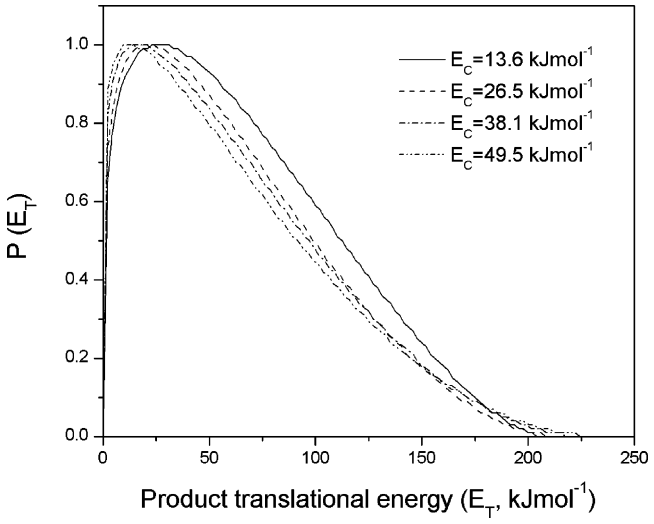

Figure 3. Center-of-mass translational energy flux distributions for reaction of dicarbon ($C_2(X^1\Sigma_g^+/a^3\Pi_u)$) with allene to form C_5H_3 radical(s) and atomic hydrogen at four collision energies.

that at least one reaction channel most likely exhibits an exit barrier. Also, the peaking of the $P(E_T)$ at lower collision energies close to the zero translation energy might indicate the existence of a second reaction pathway that involves almost no exit barrier and hence a loose exit transition state. On the basis of the center-of-mass translational energy distributions, we can calculate the fraction of the energy channeling into the translational modes of the products, $\langle E_T \rangle / E_{avl}$ (Figure 4). As the collision energy increases, the averaged fraction of the translational energy decreases from about 33 ± 2 to $28 \pm 2\%$. These data can also be fit with a linear relationship (eq 1). Also, the order of magnitude of about 30% suggests that the reaction dynamics is indirect. Recall that the tight transition state theory of Marcus predicts an increasing fraction of total available energy channeling into a vibration as the collision energy rises, if the energy is completely randomized.[23] Assuming that a constant fraction is released into the rotational energy of the C_5H_3 isomers, this would correlate with the experimentally found decreasing fraction of the total available energy channeling into the translational motion of the products. Therefore, the collision energy dependence of $\langle E_T \rangle / E_{avl}$ may indicate a complete energy randomization in the decomposing intermediates.

$$\langle E_T \rangle / E_{avl} = (0.34 \pm 0.01) - (17.6 \pm 3.1) \times 10^{-4} \times E_c \quad (1)$$

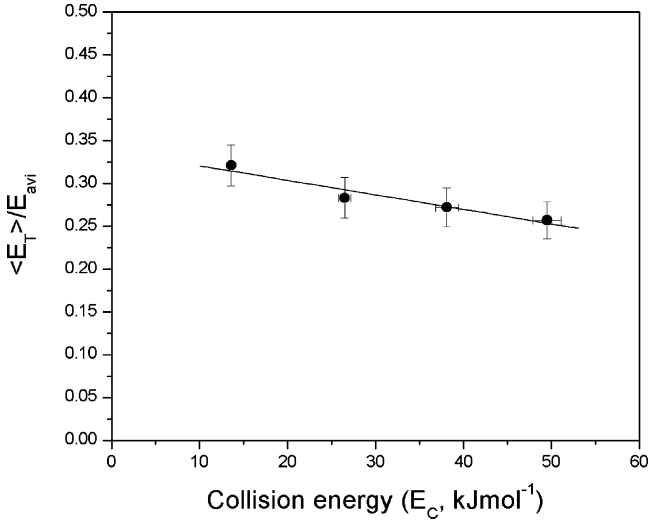

Figure 4. Collision energy dependence of the fraction of the available energy channeling into the translational modes of the products.

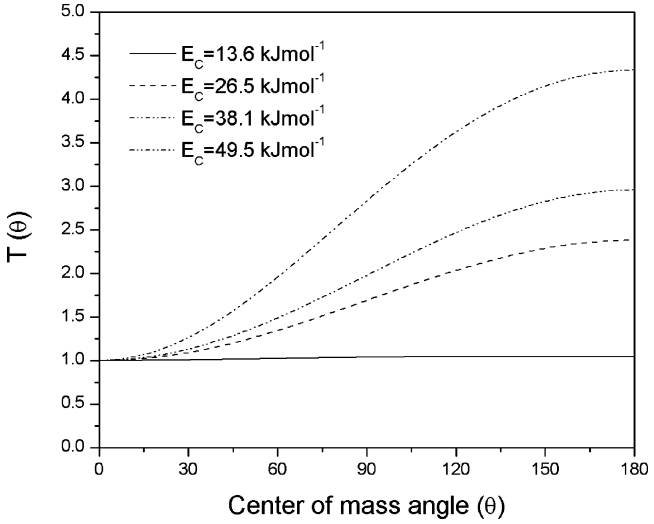

Figure 5. Center-of-mass angular distributions for the reaction of dicarbon ($C_2(X^1\Sigma_g^+/a^3\Pi_u)$) with allene to form C_5H_3 radical(s) and atomic hydrogen at four collision energies.

Center-of-Mass Angular Distributions, *T*(*θ*)s. The shape of the center-of-mass angular flux distribution, $T(\theta)$, of the atomic hydrogen loss pathway can be employed to collect important information on the chemical dynamics (Figure 5). First of all, the distributions show an intensity over the complete angular range from 0 to 180°. This finding alone suggests that the reaction dynamics are indirect and proceed via formation of C_5H_4 complex(es). At the lowest collision energy, the distribution is almost isotropic (flat), suggesting that the lifetime of the decomposing intermediate is longer than its rotational period. Note that within the error limits (Figure 6), best fits were achieved with a slightly backward scattered distribution (Figures 5 and 7). The weak polarization and hence the poor correlation between the initial and the final angular momentum can be easily understood in terms of total angular momentum conservation and angular momentum disposal.[24] Here, large reactive impact parameters lead to complex formation; also, the light departing hydrogen atom cannot carry away a significant orbital angular momentum. These results indicate an insignificant final orbital angular momentum and hence a preferential channeling of the total angular momentum into rotational excitation of the C_5H_3 product(s). However, as the collision

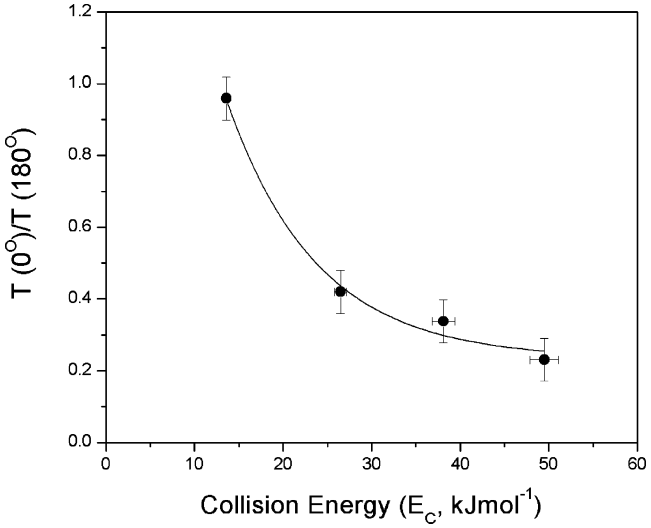

Figure 6. Collision energy dependence of the intensity ratio of the center-of-mass angular distributions at the poles, $T(0°)/T(180°)$.

energy rises, the form of the $T(\theta)$s changes dramatically to backward peaking, yielding an intensity ratio at the poles of $T(0°)/T(180°) = 0.23 \pm 0.02$ at the highest collision energy of 49.4 kJ mol^{-1}. This trend indicates that as the collision energy increases, at least one intermediate becomes short-lived (i.e., having a lifetime shorter than its rotation period). These findings are summarized in Figure 6; the collision energy dependence of the ratios of the center-of-mass angular distributions at the poles could be fit with a decaying exponential function (eq 2). The tendency can also be visualized by inspecting the center-of-mass flux contour maps shown in Figure 7.

$$T(0°)/T(180°) = (0.23 \pm 0.06) + (2.76 \pm 1.23) \times e^{-(Ec/(10.2 \pm 3.1))} \quad (2)$$

Discussion

Energetical Considerations. The inspection of the center-of-mass translational energy distributions suggests that the reaction to synthesize the C_5H_3 radical(s) plus atomic hydrogen is exoergic by 183 ± 15 kJ mol^{-1}. This high-energy cutoff can—within the error limits—account for the formation of 2,4-pentadiynyl-1 [$C_5H_3(X^2B_1)HCCCCCH_2$] and the 1,4-pentadiynyl-3 radical [$C_5H_3(X^2B_1)HCCCHCCH$] (Figure 8). Note that the computed exoergicities are 195 ± 5 and 204 ± 5 kJ mol^{-1} to form the 2,4-pentadiynyl-1 radical on the singlet and triplet surfaces, respectively, and 202 ± 5 kJ mol^{-1} to synthesize the 1,4-pentadiynyl-3 radical on the triplet manifold. On the basis of the energetics alone, we cannot decide if the 2,4-pentadiynyl-1 and/or the 1,4-pentadiynyl-3 radical is formed since their enthalpies of formation differ by only 1 kJ mol^{-1}. Therefore, we have to combine our experimental results and center-of-mass functions with the computed potential energy surfaces to resolve this question. Here, the center-of-mass angular distributions suggest indirect scattering dynamics and hence the existence of C_5H_4 intermediate(s). On the singlet surface, the calculations indicate that the addition of dicarbon to the carbon—carbon double bond of the allene molecule is barrier-less and forms a cyclic intermediate **s1**. The latter isomerizes to the D_{2d} symmetric pentatetraene molecule **s2**. Considering both energetically accessible C_5H_3 isomers, pentatetraene can solely fragment to 2,4-pentadiynyl-1 [$C_5H_3(X^2B_1)HCCCCCH_2$] via atomic hydrogen loss; the 1,4-pentadiynyl-3 radical [C_5H_3-$(X^2B_1)HCCCHCCH$] cannot be synthesized on the singlet

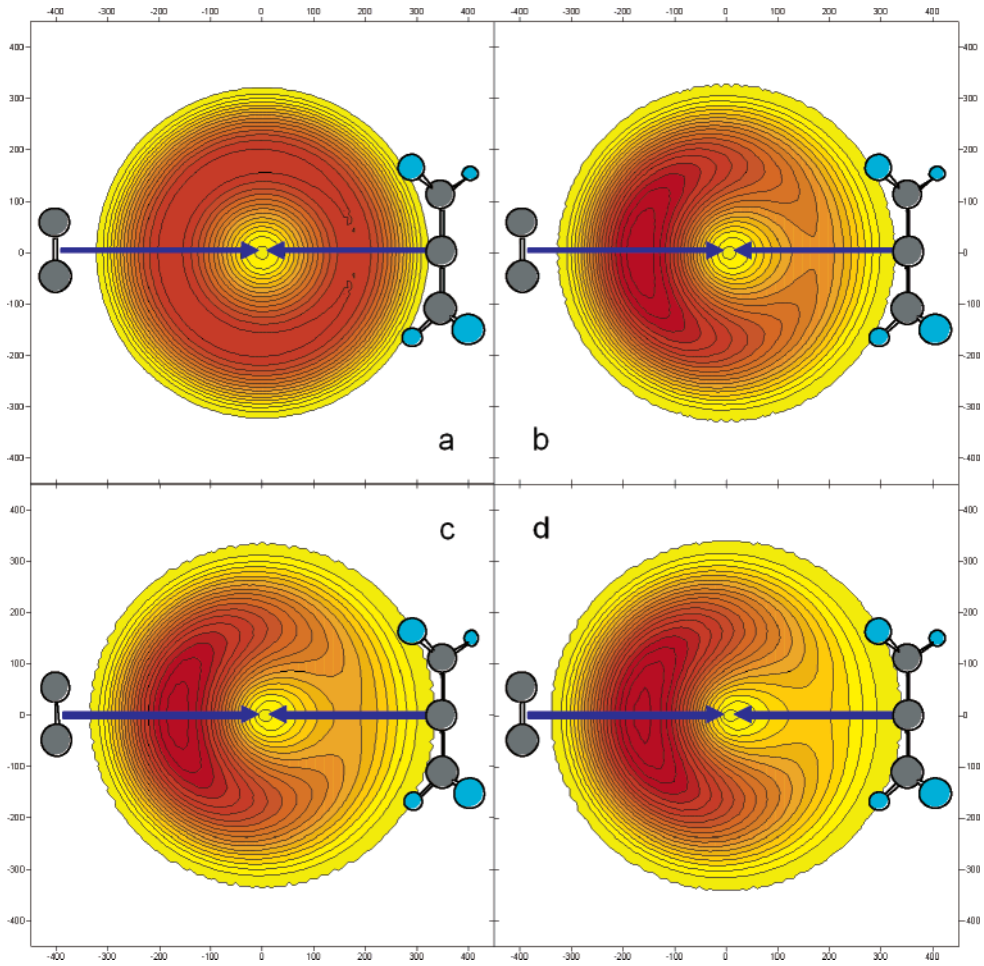

Figure 7. Flux contour plots of the C_5H_3 radical(s) reported at four different collision energies of 13.6 (a), 26.5 (b), 38.1 (c), and 49.4 kJ mol^{-1} (d). The solid lines connect data with identical fluxes.

surface; isomerizations involving H migrations in **s2** are expected to be slower than the atomic hydrogen loss.[24] On the other hand, the triplet surface can—in principle—support the generation of the less stable 1,4-pentadiynyl-3 radical as well as the energetically favorable 2,4-pentadiynyl-1 isomer via decomposing triplet intermediates **t6** and **t5**, respectively.

Angular Distribution Considerations. How can we decide now which of these C_5H_3 isomers is formed on the triplet surface? A detailed look at the center-of-mass angular distributions is helpful to resolve this issue. The singlet and triplet pentatetraene intermediates **s2** and **t5** belong to the D_{2d} and D_{2h} point groups, respectively; both isomers have C_2 axes parallel to their three principal rotational axes. Consequently, a hydrogen emission from **s2** and **t5** is expected to result in a forward−backward symmetric center-of-mass angular distribution at each collision energy since the hydrogen atoms can be converted via a 2-fold rotational axis. This means that the probability of a hydrogen atom emission from pentatetraene into $\theta°$ and $\pi-\theta°$ is equal.[24] This will result in a forward−backward symmetric center-of-mass angular distribution even if the lifetime of the fragmenting intermediate is less than its rotational period. However, our data demonstrate explicitly that the $T(\theta)$s are not symmetric: although at the lowest collision energy, $T(\theta)$ is flat and hence forward−backward symmetric; the distributions become increasingly backward scattered as the collision energy rises (Figures 5−7). Therefore, we must have at least one additional microchannel that involves a fragmenting intermediate that does not hold a C_2 rotational axis to interconvert two hydrogen atoms. A closer inspection of the pertinent potential energy surfaces verifies that **t6** might be this elusive reaction intermediate. Here, **t6** belongs to the C_s point group and can be formed via a hydrogen shift on the triplet surface from the initial collision complex **t1**; the latter is generated via a barrier-less addition of the dicarbon molecule to the terminal carbon atom of the allene molecule. Since **t6** holds no C_2 rotational axis, this intermediate can account for the asymmetry in the angular distributions at higher collision energies. Note that **t6** resides in a shallow potential energy well of only 196 kJ mol^{-1}; this suggests a lifetime of **t6** that is shorter than its rotational period. Consequently, an asymmetric center-of-mass angular distribution can be accounted for. As the collision energy rises, the lifetime of **t6** also decreases; this trend is clearly visible in the enhanced backward scattered angular distributions (Figures 5−7). Eventually, **t6** decomposes to the 1,4-pentadiynyl-3 radical [C_5H_3 (X^2B_1)HCCCHCCH]. Note that the reaction has no entrance barrier; therefore, an increase of the collision energy correlates with a decrease in the maximum impact parameter leading to complex formation. This suggests that as the collision energy increases, more **t7** (dicarbon adds to the central carbon atom of allene; this requires small impact parameters) should be formed as compared to **t1** (dicarbon adds to the terminal carbon atom of allene; this requires large impact parameters). The collision complex **t7** can isomerizes via **t3** to yield the symmetric **t5** intermediate; alternatively, **t7** undergoes ring closure to **t2**, and **t2** rearranges to **t1** and isomerizes via **t4** to **t5**. Most importantly, the low-impact parameters can account for the enhanced backward peaking as the collision energy increases. Note that the overall indirect scattering dynamics are supported by the

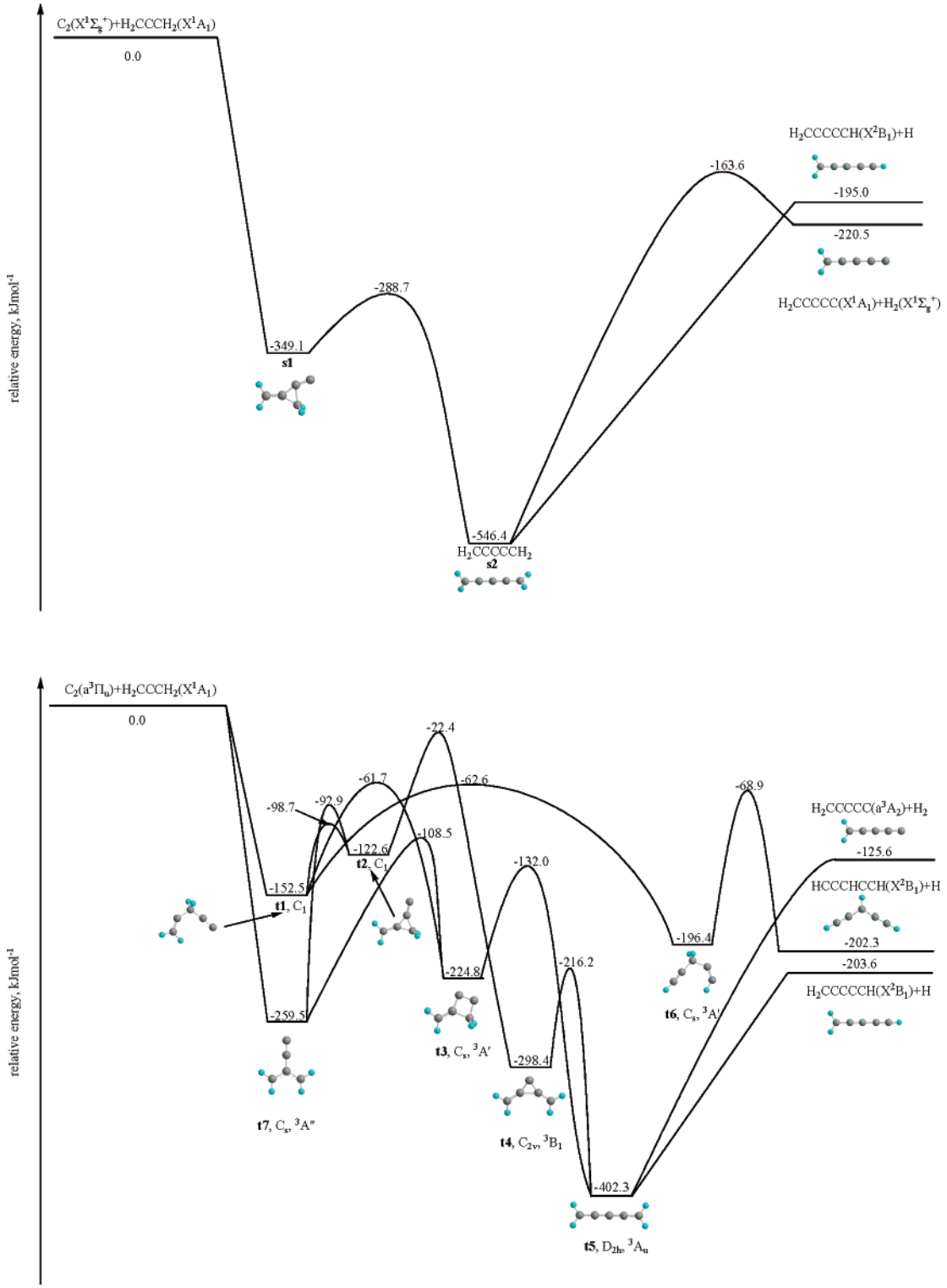

Figure 8. Simplified singlet (top) and triplet (bottom) C_5H_4 potential energy surfaces involving atomic and molecular hydrogen loss pathways in the reaction of dicarbon, $C_2(X^1\Sigma_g^+/a^3\Pi_u)$, with allene to form C_5H_3 and C_5H_2, respectively.

center-of-mass angular distributions (Figure 5), the flux contour plots (Figure 7), and the relatively small fraction of the available energy channeling into the translational motion of the products (i.e., only about 30%).

Reaction Dynamics. On the basis of these considerations, we propose the following indirect scattering dynamics involving distinct channels on the singlet (one) and triplet (two) potential energy surface. The dicarbon molecule—recall that we have dicarbon in its $X^1\Sigma_g^+$ electronic ground state as well as in its first electronically excited $a^3\Pi_u$ state—adds to the carbon−carbon double bond of the allene molecule forming a C_s symmetric **s1** collision complex on the singlet surface without entrance barrier. The latter isomerizes to pentatetraene **s2**, which fragments without exit barrier via an atomic hydrogen loss to the 2,4-pentadiynyl-1 radical $[C_5H_3(X^2B_1)HCCCCCH_2]$. Because of its symmetry and presence of C_2 axes parallel to the *A*, *B*, and *C* principal axes, the channel involving the decomposition of the singlet pentatetraene intermediate results in a forward−backward symmetric center-of-mass angular distribution at all collision energies. Detailed RRKM calculations

propose that a molecular hydrogen elimination pathway to form the H_2CCCCC (X^1A_1) cumulene carbene via a tight transition state located 47 kJ mol^{-1} above the separated products does not compete with an atomic hydrogen loss pathway. Upper limits of 2−3% were derived; the calculated rate constant for the H loss from **s2** is a factor of 55.6−33.0 higher than the rate constant for the H_2 elimination from this intermediate in the collision energy range of 0−50 kJ mol^{-1}.[24] This correlates nicely with our experimental findings and the sole detection of the atomic hydrogen loss channel; recall that the time-of-flight spectra of $m/z = 63$ ($C_5H_3^+$) and $m/z = 62$ ($C_5H_2^+$) are superimposable, demonstrating that a signal at $m/z = 62$ originates only from a dissociative ionization process of C_5H_3 in the electron impact ionizer but not from a molecular hydrogen elimination pathway.

On the triplet surface, dicarbon can add to either the terminal or the center carbon atom of the allenic carbon−carbon double bond to form **t1** and **t7**, respectively. The rovibrationally excited collision complexes **t1** and **t7** isomerize via **t3** to triplet pentatetraene (**t5**). The latter can decompose via a loose exit transition state through an atomic hydrogen loss, forming the 2,4-pentadiynyl-1 radical [$C_5H_3(X^2B_1)HCCCCCH_2$]. A molecular hydrogen elimination channel was found not to compete; preliminary RRKM calculations suggest upper limits of less than 0.1%. We also identified **t6** as the decomposing intermediate forming the 1,4-pentadiynyl-3 radical [$C_5H_3(X^2B_1)HCCCHCCH$]; this pathway was found to account for the backward scattered angular distributions at higher collision energies. Therefore, the asymmetry of the angular distributions verifies explicitly the formation of the less stable $C_5H_3(X^2B_1)HCCCHCCH$ isomer. The involvement of **t6** can also be rationalized by inspecting the involved exit transition states. Here, both **s2** and **t5** fragment barrier-less via a loose exit transition state; therefore, the center-of-mass translational energy distributions are expected to peak at zero or at least close to zero. This was not observed; best fits were achieved with distributions peaking at 3−40 kJ mol^{-1}. **t6**, on the other hand, fragmented through a tight exit transition state (Figure 8), resulting in a $P(E_T)$ peaking away from the zero translational energy (Figure 3). The exit transition state can be understood by looking at the evolution of the wave function on the course of the reverse reaction. In $HCCCHCCH(X^2B_1)$, the unpaired electron is located at a molecular orbital (MO) perpendicular to the plane of molecule and antisymmetric with respect to this plane. When atomic hydrogen adds to this structure to form **t6** ($^3A'$) on the triplet surface, two single electrons are pushed to two a′ symmetric MOs lying in the molecular plane, and one of two triple C≡C bonds in the reacting C_5H_3 radical becomes a double bond in the product. Thus, the rearrangement of the electronic structure during the reaction is very significant, and the process involves a high barrier of 133 kJ mol^{-1}. It should be noted that so far we do not have any experimental evidence of intersystem crossing (ISC) between the triplet and the singlet surfaces. Recall that if ISC from the triplet surface would be efficient, we would expect only a barrier-less decomposition of the singlet intermediates via simple bond rupture processes and hence center-of-mass translational energy distributions peaking at or close to zero translational energy. This however, has not been observed experimentally.

Alternative Exit Channels. Finally, we would like to address briefly alternative exit channels (Table 2). As outlined in Reactive Scattering Signal and TOF Spectra, we did not observe any signal at $m/z = 52$ ($C_4H_4^+$). This suggests that the pathway to form C_4H_4 plus atomic carbon $C(^3P_j)$ (channel 4) is not open.

TABLE 2: Reaction Energies for Various Reaction Pathways in Singlet Dicarbon−Allene System[a]

pathway	product	reaction energy (kJ mol−1)
1	$H_2CCCCCH(X^2B_1) + H(^2S_{1/2})$	−195
2	$HCCCHCCH(X^2B_1) + H(^2S_{1/2})$	−194
3	$H_2CCCCC(X^1A_1) + H_2(X^1\Sigma_g^+)$	−220
4	$H_2CCCCH_2(X^1A_g) + C(^3P_j)$	+23
5	i-$C_4H_3(X^2A) + CH(X^2\Pi_W)$	+83
6	$HCCCCH(X^1\Sigma_g^+) + CH_2(X^3B_1)$	−155
7	$H_2CCCC(X^1A_1) + CH_2(X^3B_1)$	+28
8	$H_2CCCC(X^1A_1) + CH_2(a^1A_1)$	+66
9	$HCCCC(X^2\Sigma^+) + CH_3(X^2A_2'')$	−23
10	$C_4(X^3\Sigma_g^-) + CH_4(X^1A_1)$	−22
11	$HCCCH_2(X^2B_2) + C_2H(X^2\Sigma^+)$	−80
12	c-$C_3H_2(X^1A_1) + C_2H_2(X^1\Sigma_g^+)$	−277
13	c-$C_3H_2(X^1A_1) + CCH_2(X^1A_1)$	−99
14	$HCCCH(X^3B) + C_2H_2(X^1\Sigma_g^+)$	−229
15	$HCCCH(X^3B) + CCH_2(X^1A_1)$	−51
16	$CCCH_2(X^1A_1) + C_2H_2(X^1\Sigma_g^+)$	−222
17	$CCCH_2(X^1A_1) + CCH_2(X^1A_1)$	−44
18	$CCCH(X^2\Pi_\Omega) + C_2H_3(X^2A)$	+15
19	c-$C_3H(X^2B_1) + C_2H_3(X^2A)$	+5
20	$C_3(X^1\Sigma_g^+) + C_2H_4(X^1A_g)$	−139

[a] Reactions of triplet dicarbons are more exoergic by 9 kJ mol^{-1}.

On the basis of the energetics and triplet surface, only **t4** could be correlated with the $H_2CCCCH_2(X^1A_g) + C(^3P_j)$ products. However, since the reaction was found to be endoergic by 23 kJ mol^{-1}, **t4** preferentially rearranged to **t5**. Considering the collision energies of up to 49.4 kJ mol^{-1}, channels 5 and 8 are too endoergic. Therefore, these pathways are closed, too. Although the reaction to form $HCCCCH(X^1\Sigma_g^+) + CH_2(X^3B_1)$ (channel 6) on the triplet surface is strongly exoergic by 155 kJ mol^{-1}, time-of-flight spectra recorded at $m/z = 50$ ($C_4H_2^+$) could be fit with a contribution from the reaction of dicarbon with allene (dissociative ionization of C_5H_3 in the electron impact ionizer; discussed in Center-of-Mass Translational Energy Distributions, $P(E_T)$**s**) and a second channel from the reaction of atomic carbon with allene forming atomic hydrogen and the 1-buten-3-yn-2-yl radical (i-$C_4H_3(X^2A')$); the latter is responsible for a signal at $m/z = 51$ (the $C_4H_3^+$parent) and the fragments at $m/z = 50$ ($C_4H_2^+$), 49 (C_4H^+), and 48 (C_4^+). A closer look at the triplet potential energy surface suggests that actually no involved intermediate **t1**−**t7** can form the diacetylene reaction product. As a matter of fact, a fragmentation of intermediates **t2**, **t5**, and **t7** would yield solely the cumulene carbene isomer $H_2CCCC(X^1A_1)$ plus $CH_2(X^3B_1)$ (channel 7). Considering the endoergicity of this reaction, our experimental data show—as expected—that this pathway does not compete with an atomic hydrogen loss from **t5**. Although channels 9 and 10 are exoergic, these pathways were not observed experimentally (see Laboratory Angular Distributions (LAB)). Here, neither the singlet nor the triplet intermediates were found to connect with the reaction products; for instance, none of the intermediates holds a methyl group to account for pathway 9. A similar argument also suggests that channels 12−16 and 18−20 are closed since none of the intermediates involved can actually connect to the potential reaction products. Channels 11 and 17 are the only feasible reaction pathways left. On the singlet surface, the formation of $CCCH_2(X^1A_1) + CCH_2(X^1A_1)$ is energetically feasible and can involve a decomposition of **s2**. However, a competing atomic hydrogen elimination is energetically more favorable by about 160 kJ mol^{-1}. Intermediate **t6**—which has been identified as the central reaction intermediate responsible for the backward peaking of the center-of-mass angular distributions—could decompose also via channel

11 to propargyl and ethynyl ($HCCCH_2(X^2B_2) + C_2H(X^2\Sigma^+)$). This pathway might compete with an atomic hydrogen loss pathway from **t6**. Our machine is currently upgraded so that experiments with a tunable electron energy of the ionizing electrons in the electron impact ionizer can be carried out; pathway 11 will be investigated in the future experimentally. Complete RRKM calculations of these pathways are published in a forthcoming paper.

Lastly, we have also investigated the possibility of direct hydrogen abstraction by dicarbon from the allene molecule to form the propargyl radical, $C_3H_3(X^2B_1)$, plus ethynyl radical, $C_2H(X^2\Sigma^+)$, products. In the triplet electronic state, the barrier for the reaction is calculated to be 27 kJ mol^{-1} at the G2M level of theory. In the singlet state, the abstraction reaction is not likely to occur. In this case, the transition state, if it exists, exhibits a strong multi-reference nature because the character of the electronic wave function changes from a closed-shell singlet for the reactants to an open-shell singlet for the products. Hence, we tried to locate this transition state at the multi-reference CASSCF/6-311G(d,p) level. We were able to find the transition state with a small active space of eight electrons distributed at seven orbitals (8,7). The calculated barrier at this level was very high and exceeded 200 kJ mol^{-1}. However, as the active space was increased to (8,8), (10,10), or (12,12), this transition state could not be reproduced, which indicated that the energy for the abstraction channel was too high and that no first-order saddle point exists. The dicarbon addition channel was much more favorable in the singlet state, and the hydrogen atom abstraction was not expected to compete with the addition.

Conclusion

We investigated the chemical dynamics of the dicarbon molecule C_2 in the $^1\Sigma_g^+$ singlet ground state and $^3\Pi_u$ in the first excited triplet state with the allene, $H_2CCCH_2(X^1A_1)$, under single collision conditions utilizing the crossed molecular beam approach. The experiments were combined with ab initio electronic structure calculations of the relevant stationary points on the singlet and triplet C_5H_4 potential energy surfaces. Our investigation suggests that the reaction dynamics are indirect on both the singlet and the triplet surface and proceed through bound C_5H_4 intermediates via barrier-less additions of the dicarbon molecule to the π electron density at the carbon−carbon double bond (singlet surface) and to the terminal as well as centered carbon atoms of the allene molecule (triplet surface). These initial collision complexes isomerize to form triplet and singlet pentatetraene intermediates ($H_2CCCCCH_2$) that decompose via atomic hydrogen loss to yield the 2,4-pentadiynyl-1 radical, $HCCCCCH_2(X^2B_1)$. These channels result in symmetric center-of-mass angular distributions. On the triplet surface, one additional channel involves the existence of a nonsymmetric reaction intermediate ($HCCCH_2CCH$), which fragments through atomic hydrogen loss to the 1,4-pentadiynyl-3 radical [C_5H_3-(X^2B_1)HCCCHCCH]; this pathway was found to account for the backward scattered angular distributions at higher collision energies. The explicit identification of two resonance-stabilized free C_5H_3 radicals (i.e., 2,4-pentadiynyl-1 and 1,4-pentadiynyl-3) suggests that these molecules can be important transient species in combustion flames and in the chemical evolution of the interstellar medium.

Acknowledgment. The experimental and theoretical work was supported by the U.S. Department of Energy−Basic Energy Sciences (DE-FG02-03ER15411 and DE-FG02-04ER15570, respectively). The construction of the crossed beams machine was also financed by the National Science Foundation (CHE-0234461).

References and Notes

(1) Melton, T. R.; Inal, F.; Senkan, S. M. *Combust. Flame* **2000**, *121*, 671.
(2) Hallin, C.; Ivanov, I. G.; Egilsson, T.; Henry, A.; Kordina, O.; Janzen, E. *J. Cryst. Growth* **1998**, *183*, 163.
(3) Woods, P. M.; Millar, T. J.; Herbst, E.; Zijlstra, A. A. *Astron. Astrophys.* **2003**, *402*, 189.
(4) Moelder, U.; Burk, P.; Koppel, I. A. *THEOCHEM* **2004**, *712*, 8104.
(5) Zahradnik, R.; Srnec, M.; Havlas, Z. *Collect. Czech. Chem. Commun.* **2005**, *70*, 559.
(6) Liang, C.; Xie, Y.; Schaefer, H. F.; Kim, K. S.; Kim, H. S. *J. Am. Chem. Soc.* **1991**, *113*, 2452.
(7) Wiberg, K. B.; Hammer, J. D.; Zilm, K. W.; Cheeseman, J. R. *J. Org. Chem.* **1999**, *64*, 6394.
(8) Zahradnik, R.; Sroubkova, L. *Helv. Chim. Acta* **2003**, *86*, 979.
(9) Markmann, A.; Worth, G. A.; Cederbaum, L. S. *J. Chem. Phys.* **2005**, *122*, 144320/1.
(10) Kaiser, R. I.; Nguyen, T. L.; Mebel, A. M.; Lee, Y. T. *J. Chem. Phys.* **2002**, *116*, 1318.
(11) Kaiser, R. I.; Lee, Y. T.; Suits, A. G. *J. Chem. Phys.* **1996**, *105*, 8705.
(12) Gu, X.; Guo, Y.; Kawamura, E.; Kaiser, R. I. *Rev. Sci. Instrum.* **2005**, *76*, 083115/1. (b) Gu, X.; Guo, Y.; Kaiser, R. I. *Int. J. Mass Spectrom. Ion Processes* **2005**, *246*, 29. (c) Gu, X.; Guo, Y.; Chan, H.; Kawamura, E.; Kaiser, R. I. *Rev. Sci. Instrum.* **2005**, *76*, 116103/1.
(13) Gu, X.; Guo, Y.; Kawamura, E.; Kaiser, R. I. *J. Vac. Sci. Technol., A* **2006**, *24*, 505. (b) Gu, X.; Guo, Y.; Zhang, F.; Kaiser, R. I. *Faraday Discuss.* **2006**, *133*, in press.
(14) Kaiser, R. I.; Mebel, A. M.; Balucani, L. Y. T.; Stahl, F.; Schleyer, P. v. R.; Schaefer, H. F. *Faraday Discuss.* **2001**, *119*, 51.
(15) Kaiser, R. I.; Stranges, D.; Lee, Y. T.; Suits, A. G. *J. Chem. Phys.* **1996**, *105*, 8721.
(16) Weiss, M. S. Ph.D. Thesis, University of California, Berkeley, Berkeley, CA, 1986. (b) Vernon, M. Ph.D. Thesis, University of California, Berkeley, Berkeley, CA, 1981.
(17) Becke, A. D. *J. Chem. Phys.* **1993**, *98*, 5648.
(18) Lee, C.; Yang, W.; Parr, R. G. *Phys. Rev. B* **1988**, *37*, 785.
(19) Mebel, A. M.; Morokuma, K.; Lin, M. C. *J. Chem. Phys.* **1995**, *103*, 7414.
(20) Purvis, G. D.; Bartlett, R. J. *J. Chem. Phys.* **1982**, *76*, 1910.
(21) Frisch, M. J. et al. *Gaussian 98*, Revision A.7. Gaussian, Inc.: Pittsburgh, PA, 1998.
(22) MOLPRO is a package of ab initio programs written by H.-J. Werner and P. J. Knowles with contributions from J. Almlöf, R. D. Amos, M. J. O. Deegan, S. T. Elbert, C. Hampel, W. Meyer, K. Peterson, R. Pitzer, A. J. Stone, P. R. Taylor, and R. Lindh.
(23) Marcus, R. A. *J. Chem. Phys.* **1975**, *62*, 1372.
(24) Kaiser, R. I. *Chem. Rev.* **2002**, *102*, 1309.